

# Measurements of $K_{e4}$ and $K^\pm \rightarrow \pi^0 \pi^0 \pi^\pm$ decays

L. Masetti \*

*Institut für Physik, Johannes Gutenberg-Universität, 55099 Mainz, Germany*

*E-mail: lucia.masetti@cern.ch*

Talk given at ICHEP06, Moscow, 2006

The NA48/2 experiment at the CERN SPS collected in 2003 and 2004 large samples of the decays  $K^\pm \rightarrow \pi^+ \pi^- e^\pm \nu_e$  ( $K_{e4}^{+-}$ ),  $K^\pm \rightarrow \pi^0 \pi^0 e^\pm \nu_e$  ( $K_{e4}^{00}$ ) and  $K^\pm \rightarrow \pi^0 \pi^0 \pi^\pm$ . From the  $K_{e4}^{+-}$  form factors and from the cusp in the  $M_{00}^2$  distribution of the  $K^\pm \rightarrow \pi^0 \pi^0 \pi^\pm$  events, the  $\pi\pi$  scattering lengths  $a_0^0$  and  $a_0^2$  could be extracted. This measurement is a fundamental test of Chiral Perturbation Theory ( $\chi PT$ ). The branching fraction and form factors of the  $K_{e4}^{00}$  decay were precisely measured, using a much larger data sample than in previous experiments.

## 1 Introduction

The single-flavour quark condensate  $\langle 0 | \bar{q}q | 0 \rangle$  is a fundamental parameter of  $\chi PT$ , determining the relative size of mass and momentum terms in the expansion. Since it can not be predicted theoretically, its value must be determined experimentally, e.g. by measuring the  $\pi\pi$  scattering lengths, whose values are predicted very precisely within the framework of  $\chi PT$ , assuming a big quark condensate [1], or of generalised  $\chi PT$ , where the quark condensate is a free parameter [2].

The  $K_{e4}^{+-}$  decay is a very clean environment for the measurement of  $\pi\pi$  scattering lengths, since the two pions are the only hadrons and they are produced close to threshold. The only theoretical uncertainty enters through the constraint [3] between the scattering lengths  $a_0^2$  and  $a_0^0$ . In the  $K^\pm \rightarrow \pi^0 \pi^0 \pi^\pm$  decay a cusp-like structure can be observed at  $M_{00}^2 = 4m_{\pi^+}^2$ , due to re-scattering from  $K^\pm \rightarrow \pi^+ \pi^- \pi^\pm$ . The scattering lengths can be extracted from a fit of the  $M_{00}^2$  distribution around the discontinuity.

## 2 Experimental setup

Simultaneous  $K^+$  and  $K^-$  beams were produced by 400 GeV energy protons from the CERN SPS, impinging on a beryllium target. The kaons were deflected in a front-end achromat in order to select the momentum band of  $(60 \pm 3)$  GeV/c and focused at the beginning of the detector, about 200 m downstream. For the measurements presented here, the most important detector components are the magnet spectrometer, consisting of two drift chambers before and

---

\*On behalf of the NA48/2 collaboration

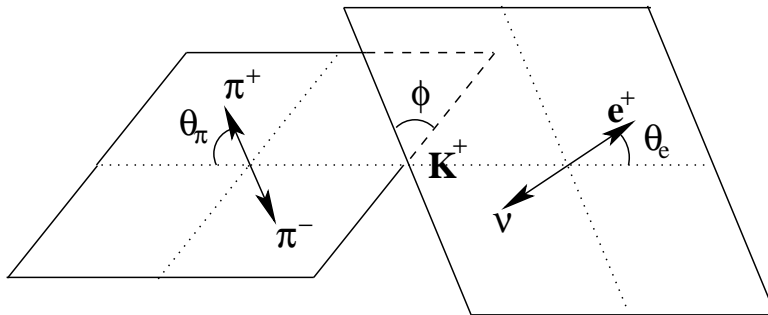


Figure 1: Topology of the  $K_{e4}$  decay.

two after a dipole magnet and the quasi-homogeneous liquid krypton electromagnetic calorimeter. The momentum of the charged particles and the energy of the photons are measured with a relative uncertainty of 1% at 20 GeV. A detailed description of the NA48/2 detector can be found in Ref. [4].

### 3 $K^\pm \rightarrow \pi^+\pi^-e^\pm\nu_e$

Analysing part of the 2003 data,  $3.7 \times 10^5$   $K_{e4}^{+-}$  events were selected with a background contamination of 0.5%. The background level was estimated from data, using the so-called “wrong sign” events, i.e. with the signature  $\pi^\pm\pi^\pm e^\mp\nu_e$ , that, at the present statistical level, can only be background, since the corresponding kaon decay violates the  $\Delta S = \Delta Q$  rule and is therefore strongly suppressed [5]. The main background contributions are due to  $K^\pm \rightarrow \pi^+\pi^-\pi^\pm$  events with  $\pi \rightarrow e\nu$  or a pion mis-identified as an electron. The background estimate from data was cross-checked using Monte Carlo simulation (MC).

#### 3.1 Form factors

The form factors of the  $K_{e4}^{+-}$  decay are parametrised as a function of five kinematic variables [6] (see Fig. 1): the invariant masses  $M_{\pi\pi}$  and  $M_{e\nu}$  and the angles  $\theta_\pi$ ,  $\theta_e$  and  $\phi$ . The matrix element

$$T = \frac{G_F}{\sqrt{2}} V_{us}^* \bar{u}(p_\nu) \gamma_\mu (1 - \gamma_5) v(p_e) (V^\mu - A^\mu)$$

contains a hadronic part, that can be described using two axial ( $F$  and  $G$ ) and one vector ( $H$ ) form factors [7]. After expanding them into partial waves and into a Taylor series in  $q^2 = M_{\pi\pi}^2/4m_{\pi^+}^2 - 1$ , the following parametrisation was used to determine the form factors from the experimental data [8, 9]:

$$\begin{aligned} F &= (f_s + f'_s q^2 + f''_s q^4) e^{i\delta_0^0(q^2)} + f_p \cos \theta_\pi e^{i\delta_1^1(q^2)} \\ G &= (g_p + g'_p q^2) e^{i\delta_1^1(q^2)} \\ H &= h_p e^{i\delta_1^1(q^2)}. \end{aligned}$$

In a first step, ten independent five-parameter fits were performed for each bin in  $M_{\pi\pi}$ , comparing data and MC in four-dimensional histograms in  $M_{e\nu}$ ,  $\cos \theta_\pi$ ,  $\cos \theta_e$  and  $\phi$ , with 1500 equal population bins each. The second step consisted in a fit of the distributions in  $M_{\pi\pi}$  (see Figs. 3,2), to extract the (constant) form factor parameters. The  $\delta = \delta_0^0 - \delta_1^1$  distribution was

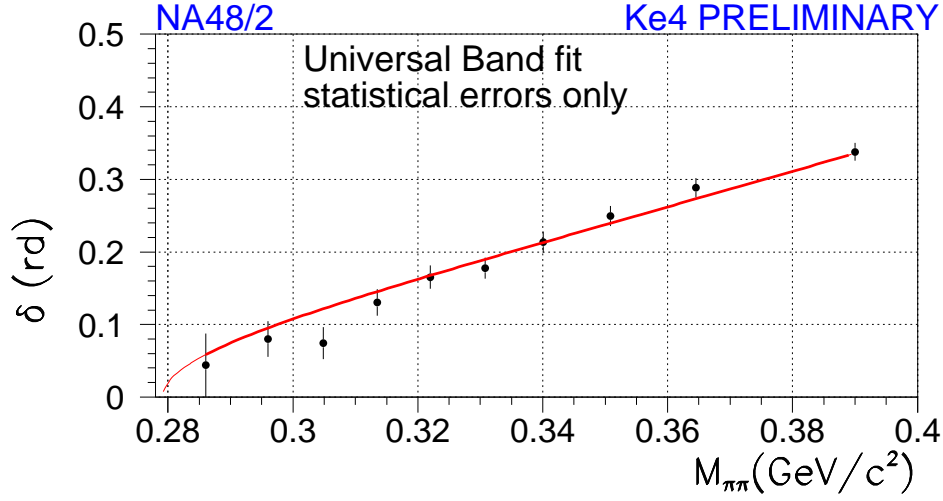


Figure 2:  $\delta = \delta_0^0 - \delta_1^1$  distribution as a function of  $M_{\pi\pi}$ . The points represent the results of the first-step fits, the line is fitted in the second step.

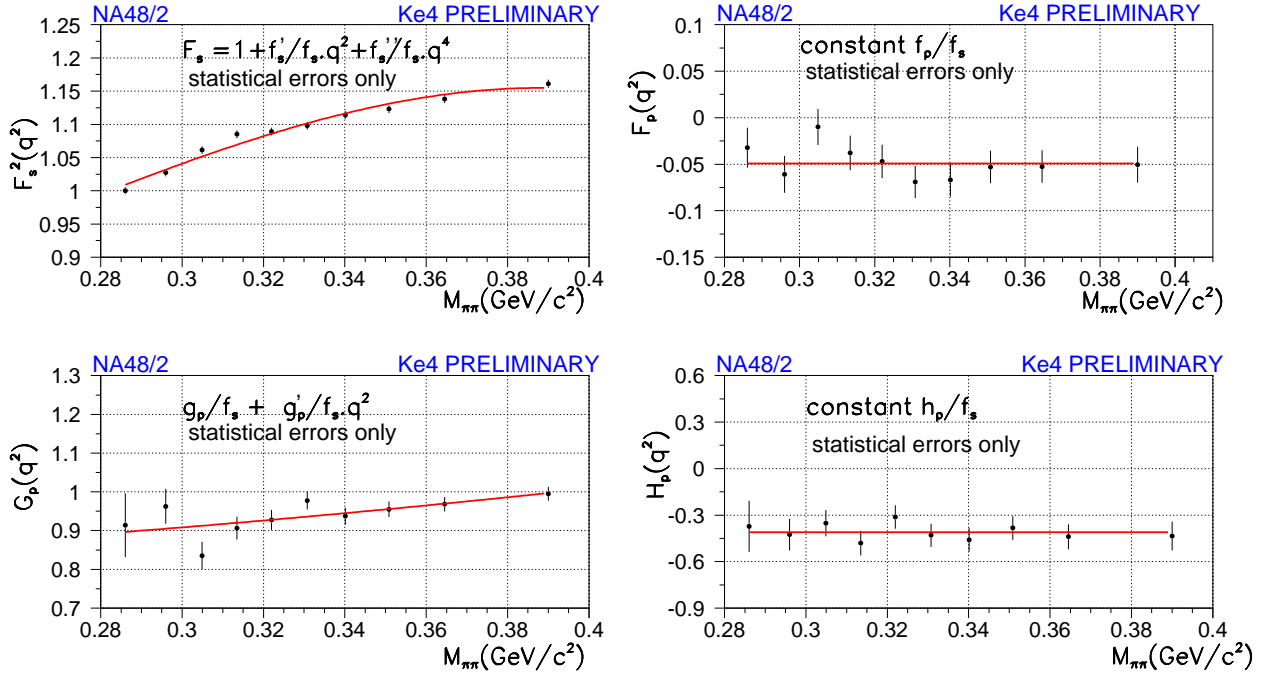


Figure 3:  $F$ ,  $G$  and  $H$  dependence on  $M_{\pi\pi}$ . The points represent the results of the first-step fits, the lines are fitted in the second step.

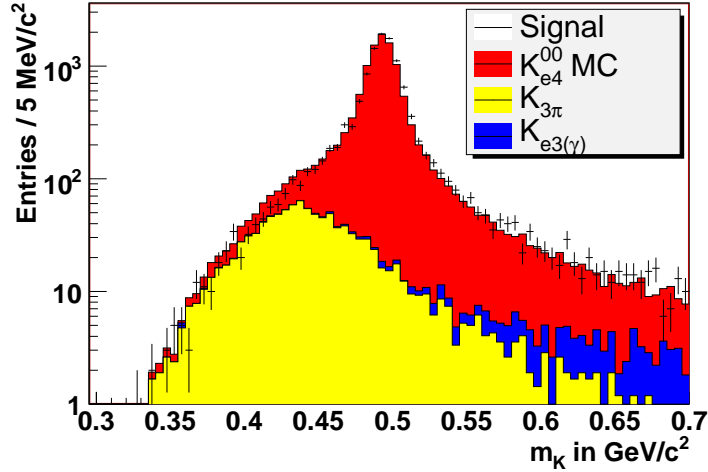


Figure 4: Invariant mass distribution in logarithmic scale of the  $K_{e4}^{00}$  events selected from the 2003 data (crosses) compared to the signal MC (red) plus physical (yellow) and accidental (blue) background.

fitted with a one-parameter function given by the numerical solution of the Roy equations [3], in order to determine  $a_0^0$ , while  $a_0^2$  was constrained to lie on the centre of the universal band. The following preliminary result was obtained:

$$\begin{aligned}
f'_s/f_s &= 0.169 \pm 0.009_{stat} \pm 0.034_{syst} \\
f''_s/f_s &= -0.091 \pm 0.009_{stat} \pm 0.031_{syst} \\
f_p/f_s &= -0.047 \pm 0.006_{stat} \pm 0.008_{syst} \\
g_p/f_s &= 0.891 \pm 0.019_{stat} \pm 0.020_{syst} \\
g'_p/f_s &= 0.111 \pm 0.031_{stat} \pm 0.032_{syst} \\
h_p/f_s &= -0.411 \pm 0.027_{stat} \pm 0.038_{syst} \\
a_0^0 &= 0.256 \pm 0.008_{stat} \pm 0.007_{syst} \pm 0.018_{theor},
\end{aligned}$$

where the systematic uncertainty was determined by comparing two independent analyses and taking into account the effect of reconstruction method, acceptance, fit method, uncertainty on background estimate, electron-ID efficiency, radiative corrections and bias due to the neglected  $M_{e\nu}$  dependence. The form factors are measured relative to  $f_s$ , which is related to the decay rate. The obtained value for  $a_0^0$  is compatible with the  $\chi PT$  prediction  $a_0^0 = 0.220 \pm 0.005$  [10] and with previous measurements [11, 12].

#### 4 $K^\pm \rightarrow \pi^0 \pi^0 e^\pm \nu_e$

About 10,000  $K_{e4}^{00}$  events were selected from the 2003 data and about 30,000 from the 2004 data with a background contamination of 3% and 2%, respectively. The background level was estimated from data by reversing some of the selection criteria and was found to be mainly due to  $K^\pm \rightarrow \pi^0 \pi^0 \pi^\pm$  events with a pion mis-identified as an electron (see Fig. 4). The branching fraction was measured, as a preliminary result from the 2003 data only, normalised to  $K^\pm \rightarrow \pi^0 \pi^0 \pi^\pm$ :

$$BR(K_{e4}^{00}) = (2.587 \pm 0.026_{stat} \pm 0.019_{syst} \pm 0.029_{ext}) \times 10^{-5},$$

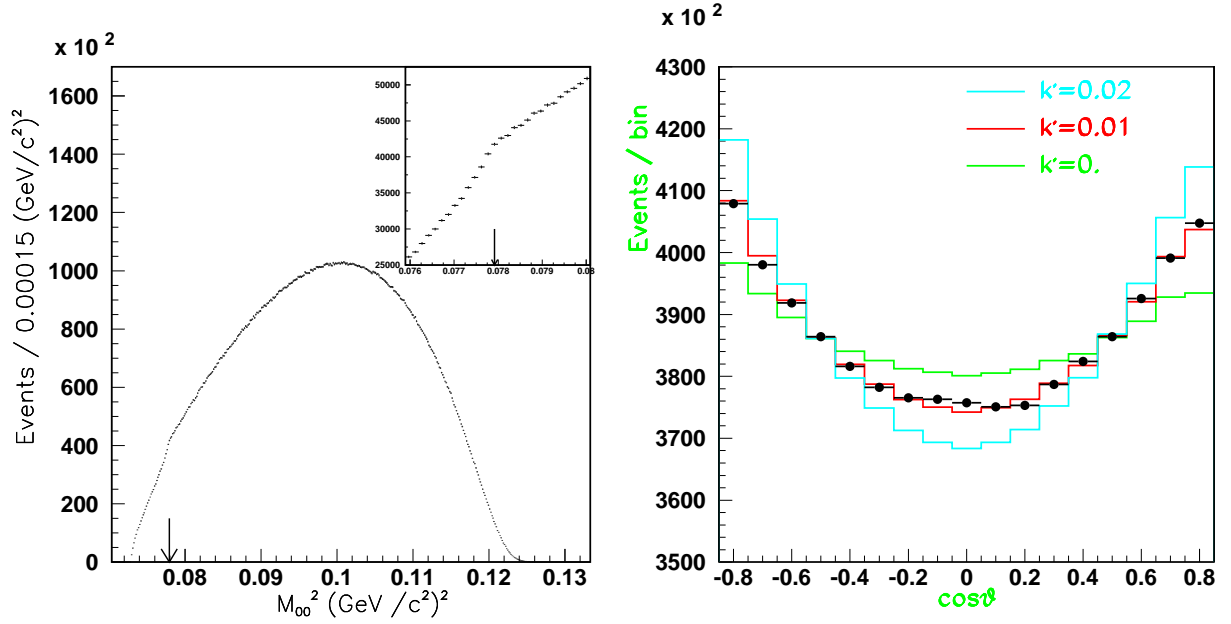


Figure 5: Left:  $M_{00}^2$  of the selection  $K^\pm \rightarrow \pi^0 \pi^0 \pi^\pm$  data events. The arrow indicates the position of the cusp. Right: angle between the  $\pi^\pm$  and the  $\pi^0$  in the  $\pi^0 \pi^0$  centre of mass system. The points represent the data, the three curves, the MC distribution for different values of  $k'$

where the systematic uncertainty takes into account the effect of acceptance, trigger efficiency and energy measurement of the calorimeter, while the external uncertainty is due to the uncertainty on the  $K^\pm \rightarrow \pi^0 \pi^0 \pi^\pm$  branching fraction. This result is about eight times more precise than the best previous measurement [13].

For the form factors the same formalism is used as in  $K_{e4}^{+-}$ , but, due to the symmetry of the  $\pi^0 \pi^0$  system, the  $P$ -wave is missing and only two parameters are left:  $f'_s/f_s$  and  $f''_s/f_s$ . Using the full data sample, the following preliminary result was obtained:

$$\begin{aligned} f'_s/f_s &= 0.129 \pm 0.036_{stat} \pm 0.020_{syst} \\ f''_s/f_s &= -0.040 \pm 0.034_{stat} \pm 0.020_{syst}, \end{aligned}$$

which is compatible with the  $K_{e4}^{+-}$  result.

## 5 $K^\pm \rightarrow \pi^0 \pi^0 \pi^\pm$

From 2003 data, about 23 million  $K^\pm \rightarrow \pi^0 \pi^0 \pi^\pm$  events were selected, with negligible background. The squared invariant mass of the  $\pi^0 \pi^0$  system ( $M_{00}^2$ ) was computed imposing the mean vertex of the  $\pi^0$ s, in order to improve its resolution close to threshold. At  $M_{00}^2 = 4m_{\pi^+}^2$ , the distribution shows evidence for a cusp-like structure (see Fig. 5) due to  $\pi\pi$  re-scattering. Fitting the distribution with the theoretical model presented in Ref. [14] and using the unperturbed matrix element

$$M_0 = A_0(1 + \frac{1}{2}g_0 u + \frac{1}{2}h' u^2 + \frac{1}{2}k' v^2),$$

the following result was obtained [15], assuming  $k' = 0$  [16]:

$$g_0 = 0.645 \pm 0.004_{stat} \pm 0.009_{syst}$$

$$\begin{aligned}
h' &= -0.047 \pm 0.012_{stat} \pm 0.011_{syst} \\
a_2 &= -0.041 \pm 0.022_{stat} \pm 0.014_{syst} \\
a_0 - a_2 &= 0.268 \pm 0.010_{stat} \pm 0.004_{syst} \pm 0.013_{theor},
\end{aligned}$$

where the  $a_0 - a_2$  measurement is dominated by the uncertainty on the theoretical model.

In a further analysis, evidence was found for a non-zero value of  $k'$  (see Fig. 5):

$$k' = 0.0097 \pm 0.0003_{stat} \pm 0.0008_{syst},$$

where the systematic uncertainty takes into account the effect of acceptance and trigger efficiency.

## References

- [1] G. Colangelo *AIP Conf. Proc.* **756**, 60 (2005).
- [2] M. Knecht *et al. Nucl. Phys. B* **457**, 513 (1995).
- [3] B. Ananthanarayan *et al. Phys. Rept.* **353**, 207 (2001).
- [4] J. R. Batley *et al. Phys. Lett. B* **634**, 474 (2006).
- [5] P. Bloch *et al. Phys. Lett. B* **60**, 393 (1976).
- [6] N. Cabibbo and A. Maksymowicz *Phys. Rev.* **137**, B438 (1965); *Ibid.* **168**, 1926 (1968).
- [7] J. Bijnens *et al. 2nd DAΦNE Physics Handbook*, 315 (1995).
- [8] A. Pais and S. B. Treiman *Phys. Rev.* **168**, 1858 (1968).
- [9] G. Amoros and J. Bijnens *J. Phys. G* **25**, 1607 (1999).
- [10] G. Colangelo *et al. Nucl. Phys. B* **603**, 125 (2001).
- [11] L. Rosselet *et al. Phys. Rev. D* **15**, 574 (1977).
- [12] S. Pislak *et al. Phys. Rev. D* **67**, 072004 (2003).
- [13] S. Shimizu *et al. Phys. Rev. D* **70**, 037101 (2004).
- [14] N. Cabibbo and G. Isidori *JHEP* **0503**, 021 (2005).
- [15] J. R. Batley *et al. Phys. Lett. B* **633**, 173 (2006).
- [16] S. Eidelman *et al. Phys. Lett. B* **592**, 1 (2004).